Appl. Phys. B 70, 721–730 (2000) / Digital Object Identifier (DOI) 10.1007/s003400000297

Applied Physics B
Lasers
and Optics

Micromanipulation of neutral atoms with nanofabricated structures

D. Cassettari[1], A. Chenet[1], R. Folman[1], A. Haase[1], B. Hessmo[1,2], P. Krüger[1], T. Maier[3], S. Schneider[1], T. Calarco[4,5], J. Schmiedmayer[1]

[1] Institut für Experimentalphysik, Universität Innsbruck, 6020 Innsbruck, Austria
[2] Department of Quantum Chemistry, Uppsala University, 75120 Uppsala, Sweden
[3] Institute für Festkörperelektronik, Floragasse 7, 1040 Wien, Austria
[4] Institut für Theoretische Physik, Universität Innsbruck, 6020 Innsbruck, Austria
[5] ECT∗, Villa Tambosi, Strada delle Tabarelle 286, 38050 Villazzano, Italy

Received: 20 December 1999/Revised version: 7 March 2000/Published online: 5 April 2000 –

Abstract. A large variety of trapping and guiding potentials can be designed by bringing cold atoms close to charged or current carrying material objects. We describe the basic principles of constructing microscopic traps and guides and how to load atoms into them. The simplicity and versatility of these methods will allow for miniaturization and integration of atom optical elements into matter-wave quantum circuits on *Atom Chips*. These could form the basis for robust and widespread applications in atom optics, ranging from fundamental studies in mesoscopic physics to possibly quantum information systems.

PACS: 03.75.Be; 03.65.Nk

In electronics and light optics, miniaturization of components and integration into networks has led to new, very powerful tools and devices, for example in quantum electronics [1] or integrated optics [2]. It is essential for the success of such designs that the size of the structures is, at least in one dimension, comparable to the wavelength of the guided wave. Similarly we anticipate that atom optics [3], if brought to the microscopic scale, will give us a powerful tool to combine many atom optical elements into integrated quantum matter-wave circuits.

Such microscopic scale atom optics can be realized by bringing cold atoms [4, 5] close to nanostructures [6–8]. Atoms can be cooled so as to reach a de Broglie wavelength λ_{dB} of 100 nm or larger, which is in the regime where one can easily design and build material structures of such size using techniques from the semiconductor industry.

Microscopic potentials for neutral atoms can be constructed using:

(i) The electric interaction between a neutral, polarizable atom and a charged nanostructure, where the potential is $V_{\mathrm{el}} = -\frac{1}{2}\alpha_{\mathrm{el}} E^2$.
(ii) The magnetic interaction between the atomic magnetic moment μ and a magnetic field B, which is described by the potential $V_{\mathrm{mag}} = -\boldsymbol{\mu} \cdot \boldsymbol{B}$.

These potentials can also be combined with traditional atom optical elements like atom mirrors and evanescent light fields. A variety of novel atom optical elements like quantum wells, quantum wires and quantum dots for trapping and guiding neutral atoms can then be constructed on the microscopic scale. These elements can be further combined to form more complex structures, for example, coherent beam splitters and microscopic interferometers[1].

Having the atoms trapped or guided – well localized near the surface – will allow the integration of atom optics and light optics with, for example, light cavities and wave guides fabricated on the surface. These can be used to address or detect individual neutral atoms in these quantum wires or quantum dots. For example, atoms can be shifted in and out of resonance by applying additional fields using supplementary electrodes. Integration with other technologies such as microelectronics and cavity QED on the surface should allow one to manipulate and detect the external (motional) and internal states of atoms.

In such microscopic traps, atoms can in principle be manipulated individually. This will open the possibility for "quantum engineering", i.e. preparing and modifying atomic quantum states in a controlled way [9], which is one of the key ingredients for quantum information processing [10]. Neutral atoms have a weaker dissipative coupling to the environment than other already proposed systems for quantum computation, and are therefore a promising candidate for the development of a scalable quantum processor [11]. Using the techniques described later in this text, one should be able to trap atoms close to a surface with submicron precision. By arranging such microtraps in a periodic array structure, several atoms could be handled at once, and parallelism could be exploited for efficient error correction in order to further reduce decoherence. Even ground state cooling is not an absolute need: a fidelity close to 1 was found in a simulation of quantum

[1] For example, a robust microfabricated atomic Sagnac-interferometer would be the instrument of choice for rotation measurements.

gates assuming a temperature of some micro-Kelvin in one dimension [11].

The paper is organized as follows: In Sect. 1 we present the design principles of microscopic traps and guides mounted on a surface, show how to load the atoms into successively smaller structures and how to transfer the atoms between different traps and guides. In Sect. 2 we describe methods for transferring atoms from a MOT to magnetic traps on a chip and give examples of our experiments. Section 3 discusses the possibilities of mesoscopic atom optics for fundamental physics and quantum information processing.

1 Microscopic traps

Magnetic trapping [12] of neutral particles is a well developed tool for experiments with cold atoms and it has been used in diverse applications such as atom optics [3], the study of ultra-cold collisions [13], and the creation of Bose–Einstein Condensates [5].

An atom with magnetic moment $\boldsymbol{\mu}$ experiences the potential $V = -\boldsymbol{\mu} \cdot \boldsymbol{B}$. In general the vector coupling $\boldsymbol{\mu} \cdot \boldsymbol{B}$ results in a very complicated motion for the atom. However, in most cases the Larmor precession (ω_{L}) of the magnetic moment is much faster than the apparent change of direction of the magnetic field in the rest frame of the moving atom (ω_{B}) and an adiabatic approximation can be applied. The magnetic moment then follows adiabatically the direction of the field and the atom can be described as moving in a scalar potential $V = -\mu_{\parallel} B$, where $\mu_{\parallel}$ is the projection of $\boldsymbol{\mu}$ on $\boldsymbol{B}$.

Since the Earnshaw theorem forbids a local maximum of the magnetic field in free space [14, 15] the most common magnetic traps are *weak-field-seeking* traps[2] working for atoms in weak-field-seeking states.

1.1 Design principle for microtraps

To compute $|B|$ when superposing two magnetic fields, one has to consider both the magnitude of the fields and their direction. This gives an additional degree of freedom for creating trapping potentials by separating the structures responsible for the trap depth and the field gradient. This "superposition principle" can be applied to many magnetic devices, for example micromagnets in a homogeneous field would show similar characteristics [18, 19].

A quadrupole potential can be built by superposing a homogeneous magnetic field with the field generated by a thin current carrying wire [21] (Fig. 1). The trap depth is given by the homogeneous field, the gradient and curvature by the magnetic field from the wire. The minimum of the combined field will be located where the homogeneous bias field and the field of the wire have the same magnitude but opposite direction. Since magnetic fields change at a length scale of the same order as the distance from the current, this is also the characteristic size of the trap [22]. Using more complicated wire patterns, many different trap and guide geometries can be created (see for example [22–28]).

[2] *Strong field seeking* traps require the source of the magnetic field to be located inside the trapping region. A possible realization of such a trap is a current carrying wire [12, 16–20] with the atom orbiting around it.

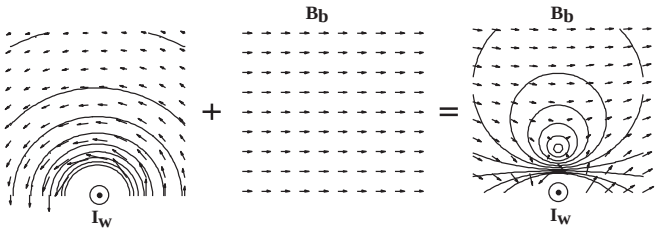

Fig. 1. Design principle of magnetic traps by obtained superimposing a homogeneous field with the field of a microscopic structure. The field from the wire and the homogeneous bias field add up to a quadrupole field around the point where the fields cancel [21]

These traps and guides have an interesting property: For given homogeneous bias field $\boldsymbol{B}_{\mathrm{b}}$ and wire current I_{w}, the magnetic field gradient scales with $B_{\mathrm{b}}^2/I_{\mathrm{w}}$. Having the trap depth fixed by the bias field, a compression of the trap can be accomplished by decreasing the current in the wire.

Steep (microscopic) potentials can therefore be realized using very small material structures (e.g. thin filaments). The extreme fragility of such structures would demand mounting them on a surface. Once mounted, even thin wires can sustain strong electric forces and support large currents because they can be cooled efficiently [22–25]. Moreover, one has the advantage that nanofabrication technologies can be used in order to realize complex atom optical circuits on the smallest scale. Having everything nanofabricated to high precision also ensures that all the fields are perfectly aligned and will make complex experiments much more robust.

Because of their similarity to quantum electronics [1], we will call structures that provide one-dimensional confinement, i.e. where atoms are allowed to move freely along the surface, a *quantum well*. Structures with two-dimensional confinement, i.e. a microscopic atom guide, will be called a *quantum wire*; three-dimensional confinement will be called a *quantum dot*.

We will now briefly discuss some options for matter–wave optics above surfaces with magnetic and electric potentials.

1.1.1 Guides.

Side Guide. The simplest way to implement these design principles is the *side guide* [18–20, 26], formed by adding the constant bias field $\boldsymbol{B}_{\mathrm{b}}$ in a direction orthogonal to the wire. The bias field cancels exactly the circular magnetic field of the wire along a line parallel to the wire at a distance

$$r_0 = \frac{\mu_0}{2\pi} \frac{I_{\mathrm{w}}}{B_{\mathrm{b}}} .$$

Around this line the modulus of the magnetic field increases in all directions and forms a tube with a magnetic field minimum at its center. Atoms in the weak-field-seeking state can be trapped in this two-dimensional quadrupole field and guided along the side of the wire, hence the name *side guide*.

At the center of the trap the magnetic field gradient is

$$\left.\frac{\mathrm{d}B}{\mathrm{d}r}\right|_{r_0} = \frac{2\pi}{\mu_0} \frac{B_{\mathrm{b}}^2}{I_{\mathrm{w}}} .$$

If the bias field is orthogonal to the wire, the two fields cancel exactly [21]. Close to the zero point of the magnetic field, trapped atoms can be lost by Majorana transitions between the trapped and untrapped spin states. However, this problem can be circumvented by adding a small B-field component along the wire direction. By choosing appropriate magnetic bias fields the guiding potential and its characteristics can be tailored at will. With an additional field $B_{\rm ip}$ along the wire a Ioffe–Pritchard guide is obtained, which is characterized by the curvature in the radial direction

$$\left.\frac{\mathrm{d}^2 B}{\mathrm{d}r^2}\right|_{r_0} = \left(\frac{2\pi}{\mu_0}\right)^2 \frac{B_{\rm b}^4}{B_{\rm ip} I_{\rm w}^2}\,.$$

When mounting the wire on a surface, the bias field has to be parallel to the surface. It is interesting to note that the bias field for the side guide can be formed by two additional wires on each side of the guiding wire, carrying current in the opposite direction to the guiding wire (Fig. 2). This is especially interesting because the wires can be mounted on the same chip, and a self-sufficient guide can be obtained.

Examples of typical guiding parameters are given in Table 1. For example, trap frequencies of the order of 1 MHz or higher can be achieved with moderate currents and bias fields. The guided atoms are then located a few μm above the surface.

Our experiments demonstrating the side guide using free standing wires [18–20] and with wires on an *Atom Chip* with external and on-board bias field [25] will be reviewed briefly in Sect. 2.

Two-Wire Guide. A different way to create a guide is by using two wires with currents flowing in opposite directions, with a bias field which has a component $B_{\rm b}$ orthogonal to the plane containing the two wires (Fig. 2) (see also [24]). If there is an additional bias field $B_{\rm ip}$ applied along the wires, a Ioffe–Pritchard guide is obtained.

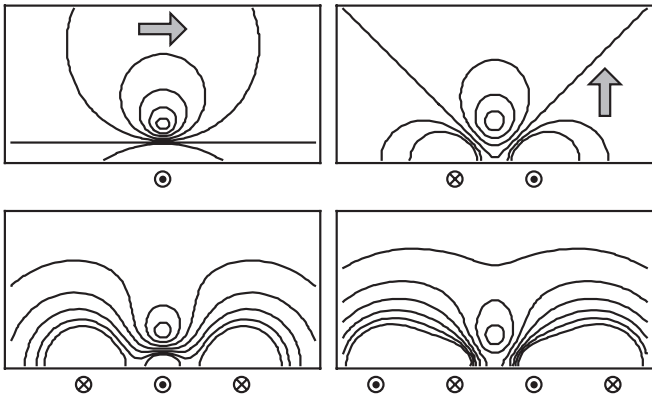

Fig. 2. *Upper left picture* shows the potential for a side guide generated by one wire and an external bias field along the surface where the wire sits. The external bias field can be replaced by two extra wires. This is illustrated in the *lower left picture*. The *second column* shows the field configuration for a two-wire guide with an external bias field perpendicular to the surface of the wires. This external bias field may also be replaced by surface-mounted wires

Table 1. Typical potential parameters for quantum wires, based on tested *Atom Chip* components: *(top)* The *side guide* created by a thin current carrying wire mounted on a surface with an added bias field parallel to the surface but orthogonal to the wire, and *(bottom)* the *two wire guide* created by two thin current carrying wires mounted on a surface with an added bias field orthogonal to the plane of the wires. In this example the two wires are 10 μm apart (see also Fig. 2)

Side guide

Atom	Wire Current /mA	Bias fields $B_{\rm b}$ /G	Bias fields $B_{\rm ip}$ /G	Potential Depth /mK	Potential Distance /μm	Ground state Freq. /kHz	Ground state Size /nm
Li	10	10	1	0.6	2	220	80
Li	100	40	4	2.4	5	180	90
Li	100	200	4	13	1	4500	18
Rb	10	10	1	0.6	2	64	42
Rb	100	40	4	2.4	5	52	50
Rb	100	200	4	13	1	1300	10

Two wire guide

Atom	Wire Current /mA	Bias fields $B_{\rm b}$ /G	Bias fields $B_{\rm ip}$ /G	Potential Depth /mK	Potential Distance /μm	Ground state Freq. /kHz	Ground state Size /nm
Li	10	5	1	0.3	4	44	180
Li	100	40	4	2.4	5	180	90
Li	600	200	5	13	6	790	40
Rb	10	5	1	0.3	4	12	100
Rb	100	50	5	3	4	55	45
Rb	600	200	5	13	6	220	20

The field generated by the wires compensates the bias field $B_{\rm b}$ at a distance

$$r_0 = \frac{d}{2}\sqrt{\frac{2\mu_0}{\pi}\left(\frac{I_{\rm w}}{B_{\rm b}}\right)\frac{1}{d} - 1}\,,$$

where d is the distance between the two wires. When $B_{\rm b} > 2\mu_0 I_{\rm w}/\pi d$ the field from the wires is not capable of compensating the bias field. Two side guides are then obtained, one along each wire in the plane of the wires.

In the case where $B_{\rm b} < 2\mu_0 I_{\rm w}/\pi d$ and where $B_{\rm b}$ has no component along the wire, the relevant quantity for characterizing the guide is the gradient in the confining directions, given by

$$\left.\frac{\mathrm{d}B}{\mathrm{d}r}\right|_{r_0} = \frac{2\pi}{\mu_0}\frac{B_{\rm b}^2}{I_{\rm w}}\sqrt{\frac{2\mu_0}{\pi}\left(\frac{I_{\rm w}}{B_{\rm b}}\right)\frac{1}{d} - 1}\,.$$

If there is a field component $B_{\rm ip}$ along the wire, the position of the guide is unchanged. The relevant quantity near the potential minimum is then the curvature in the radial direction:

$$\left.\frac{\mathrm{d}^2 B}{\mathrm{d}r^2}\right|_{r_0} = \left(\frac{2\pi}{\mu_0}\right)^2 \frac{B_{\rm b}^4}{B_{\rm ip} I_{\rm w}^2}\left[\frac{2\mu_0}{\pi}\left(\frac{I_{\rm w}}{B_{\rm b}}\right)\frac{1}{d} - 1\right].$$

1.1.2 Beam splitters. The wire guides described in the previous section can easily be combined to build more complicated atom optical elements for guided atoms. The simplest of these are beam splitters (Figs. 3–5). These can be constructed using both the one wire and the two wire guides.

Such a beam splitter for guided atoms behaves quite differently from an ordinary optical beam splitter. The beam splitting is best described as a scattering process from incoming modes to outgoing modes. The beam splitter is coherent if it is impossible to tell, by looking at the incoming mode, which way the atom goes. This is equivalent to the case with a photon propagating through a double slit.

If the potential is spatially symmetric relative to the axis of the incoming guide throughout the splitting process, symmetry conservation ensures that modes are split with equal amplitudes between the outgoing guides. Therefore, a symmetric Y-configuration enables an equal splitting over a wide range of experimental parameters due to its inherent symmetry, where by inherent we mean that the potential symmetry is maintained for different magnitudes of current and bias field, and for different incoming transverse modes. Coherent splitting in such a symmetric Y-configuration was also numerically confirmed in model calculations for up to the first 40 modes.

This equal splitting ratio, arising from the inherent symmetry of a Y, is an advantage over beam splitter designs for guided matter waves which rely on tunneling [29]. There, the splitting ratio depends strongly on the tunneling probability which will be vastly different for different propagating modes and barrier structures which in turn are changing with current and bias field.

Side guide beam splitters. The simplest beam splitter can be formed by a Y-shaped wire and a bias field parallel to the plane of the Y, orthogonal to the incoming wire (Fig. 3a). Atoms will be guided above the wires: For example, sending a current through one arm of the Y-beam splitter, the atoms will be guided along this arm. By sending the current through both arms the atomic wave function can be split and atoms are guided in both outgoing guides.

Looking closer at the beam splitter potential we see that there are three main guides, each corresponding to an incoming or outgoing current. Furthermore, the splitting point of these guides is *not* the geometric splitting point of the current-carrying wires (see Figs. 3a and 4). There is an additional guide leaving the splitting point of the potential going back towards the geometric splitting point of the current-carrying wires. This guide is located exactly underneath the incoming guide. Between the geometric splitting point of the wire and the potential splitting point these two guides have distances

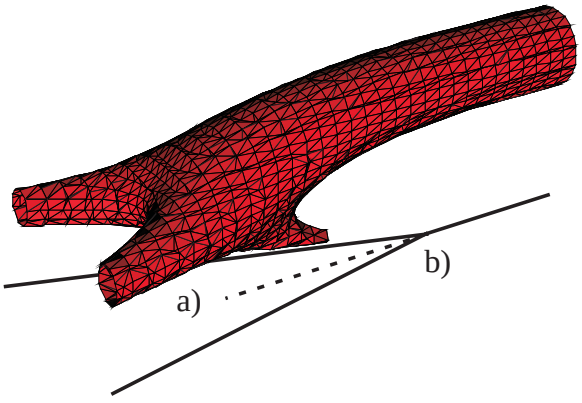

Fig. 4. Equipotential surface of a one-wire Y-beam splitter. The actual splitting point of the potentials (a) is shifted with respect to the geometric splitting point of the current carrying wires (b). Between these two splitting points the additional guide is visible. Note that this guide leads down to the geometric splitting point, even if the plot fails to show this

r_+ and r_- from the surface, respectively. $r_\pm$ is given by:

$$r_\pm = \frac{\mu_0}{4\pi}\frac{I_\mathrm{w}}{B_\mathrm{b}} \pm \sqrt{\left(\frac{\mu_0}{4\pi}\frac{I_\mathrm{w}}{B_\mathrm{b}}\right)^2 - \left(\frac{d}{2}\right)^2},$$

with d being the distance between the outgoing wires. The minima merge when the second term vanishes. This happens when $d_\mathrm{split} = \frac{\mu_0}{2\pi}\frac{I_\mathrm{w}}{B_\mathrm{b}}$.

The propagation of a de Broglie wave in this potential is rather complicated. There is only half the current flowing in the two outgoing wires, compared to the incoming wire, resulting in a tighter guide. Hence, the guiding potentials have different mode structures in incoming and outgoing guides. This mismatch causes reflections back into the incoming guide. Additional complications arise from the complicated shape of the potential near the splitting point.

A geometry eliminating such a problem is a beam splitter made from two wires coming close to each other, but not touching (Fig. 5a). When the wires are separated by a distance large compared to the distance of the guide from the wire, this configuration gives two separated guides. When the wires approach each other the two guides come closer. Depending on the bias field and the distance between the wires either a tunneling barrier ($d > d_\mathrm{split}$) or a single guide ($d = d_\mathrm{split}$) forms. When the wires separate after the closest approach

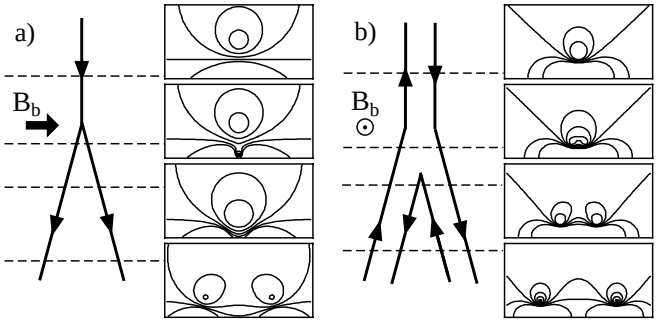

Fig. 3. a Wire layout and the potential for a Y-shaped beam splitter. The start of the additional guide (see text) is visible in the second potential plot. **b** A two wire beamsplitter creating a pure Y-shaped beam splitting potential

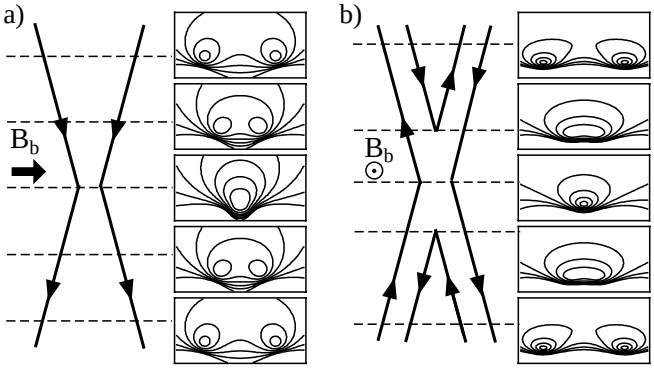

Fig. 5. Wire layout and potentials for one and two wire four-port beam splitters

two distinct guides form again (Fig. 5a). However, this beam splitter does not have the required symmetry along the incoming guide. Such an X-shaped beam splitting potential with a tunneling barrier as splitting mechanism was discussed by E. Anderson et al. [29].

Two-Wire Beam Splitter. Similarly, one can form beam splitters using the two-wire guide. A Y-shaped beam splitter can easily be formed as shown in Fig. 3b. In such a design the problem with the additional potential minimum below the incoming guide does not arise and the problem of different guide height and compression in the split arms and the incoming lead can also be circumvented. Symmetry of this Y-shaped beam splitting potential ensures coherent splitting for many propagating modes.

By combining two Y-shaped beam splitters into an X-shaped structure (Fig. 5b) one obtains a device with four ports, two input channels and two output channels. The symmetry with respect to the incoming guide is broken and coherent splitting will be much harder to obtain for many propagating modes simultaneously.

An overview of our early experiments exploring these beam splitting potentials using macroscopic free standing Y-shaped wire [19, 30] is given in Sect. 2.

1.1.3 Traps. Three-dimensional microfabricated magnetic traps can be created by bending the current-carrying wire of the side guide [26, 31]. The magnetic field from the bent leads creates 'endcaps' for the wire guide, confining the atoms along the wire. The size of the trap along this axis is then given by the distance between the endcaps. Here we describe two different geometries:

(1) Bending the wire into a "U"-shape (Fig. 6b) creates a magnetic field which rotates in direction over 180° in each plane parallel to the "U". When superimposing a homogeneous bias field one can always find a point where the two magnetic fields cancel exactly. Consequently, there is always a zero point in the trapping potential. If the bias field is parallel to the bent leads, one obtains a three-dimensional quadrupole trap [32].

(2) One can break the 180° rotation of the magnetic field vectors by bending the wire ends into opposite directions forming a "Z" (Fig. 6c). The magnetic field vectors in a plane parallel to the Z rotate by less then 90° and then back. Consequently, one can find directions of the external bias field where there are no zeros in the trapping potential. This is the case when the bias field is parallel to the leads. This configuration creates an Ioffe–Pritchard-type trap. The axial components created by the magnetic field of the two leads, bent in opposite directions, add up at the center and the potential minimum is not zero. This additional feature of the Z-trap will prevent the atoms from making Majorana transitions when trapped.

The potentials for the U- and the Z-trap scale similarly as for the side guide, but the finite length of the central bar and the directions of the leads have to be accounted for. Simple scaling laws only hold as long as the distance of the trap from the central wire is smaller than the length of the central bar [31].

Similar small wire-based magnetic traps were recently realized by Denschlag et al. [19, 20] and Fortagh et al. [33] by

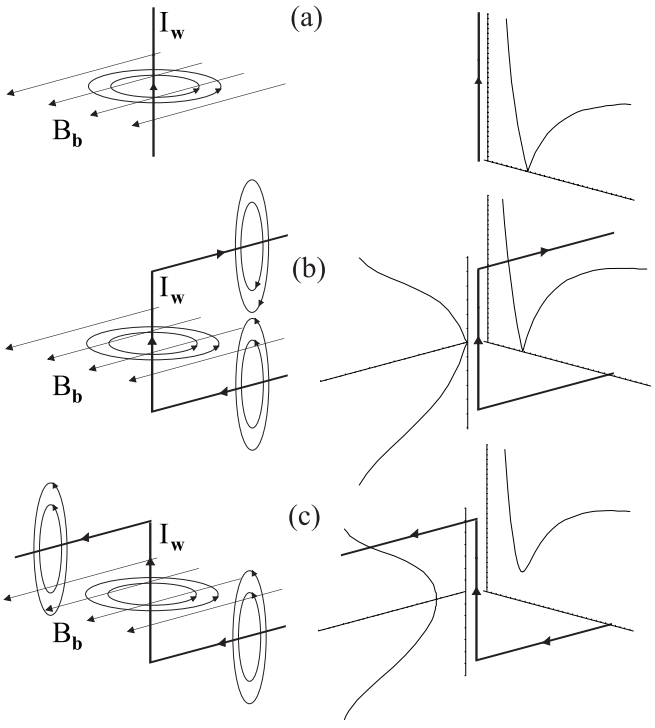

Fig. 6a–c. Creating wire traps: The *left column* shows the geometry of various trapping wires, the currents and the bias fields. The *right column* shows the radial trapping potential, and in (b) and (c) also the axial potential. **a** The side guide: Adding a homogeneous magnetic field (B_b) perpendicular to a current carrying wire (I_w) creates a two-dimensional quadrupole guide along the wire. **b** A "U"-shaped wire results in confinement in the axial direction. The field configuration is similar to a three-dimensional quadrupole field with a zero in the trapping center. **c** For a Z-shaped wire a Ioffe-Pritchard-type trap is obtained

superposing an inhomogeneous bias field. Even more elaborate designs for traps than the ones described here can be envisioned (see for example [22]). Similarly, one can design guides and traps by replacing the current-carrying wires by adequately shaped permanent magnetic structures. For example, a magnetic tip superposed by a bias field allows the creation of steep microscopic traps as recently demonstrated by V. Vuletic et al. [34] and magnetic edges could be used to build guides [35].

1.1.4 State dependent traps for quantum information. The magnetic guides and traps can be modified by combining electric and magnetic interaction, thereby creating state dependent tailored potentials. For example, additional supplementary electrodes located close to a guiding wire can be used to modify the guiding potential on demand. One can easily imagine designing switches, gates, modulators etc. for guided atoms.

This is especially interesting since it can lead to implementing quantum information processing with neutral atoms in microscopic trapping potentials. In this case logical states are identified with atomic internal levels $|a\rangle$ and $|b\rangle$. Single-qubit operations are induced as transitions between them by external fields [9, 11]. Two-qubit gates can be realized by state dependent collisions between atoms, controlled via the trapping potential: Initially, two atoms (each carrying a qubit) are trapped in two separate potential wells, whose centers are sufficiently far apart so that the particles do not interact. Then

the form of the potential wells is changed such that there is some overlap of the atomic wave functions of the two atoms; the particles interact with each other, and then the potential is restored to the original situation. The collisional interaction induces a phase shift in the two-atom wave function. Such a process provides a quantum logical gate if the collisional phase is sensitive to the atomic internal state. Therefore, the potential shape has to be both time and state dependent.

One possibility to achieve such time and state dependent microscopic potentials is by choosing two hyperfine states with different magnetic moments as the basis of the qubit. Adding an electric field $\boldsymbol{E}$ to the magnetic microtrap introduces a Stark shift energy $V_{\rm el} \approx -\frac{1}{2}\alpha_{\rm el}|\boldsymbol{E}|^2$, ($\alpha_{\rm el}$ is the atomic polarizability) which is independent of the hyperfine sublevel. Since the two hyperfine states have a different interaction strength with the magnetic field but an (approximately) equal interaction strength with the electric field, a combination of both interactions allows for state dependent manipulation of the confining potentials as illustrated below.

A simple configuration, showing such a controllable state-dependence, is a magnetic wire guide or trap, plus a charged wire fabricated on the surface, perpendicular to the current carrying wire (for single-layer design, the charge carrying wire can be split into two parts at the crossing with the current carrying one). The electrostatic potential provides confinement along the direction parallel to the side guide, and also shifts the trapping minimum towards the surface, possibly breaking the potential barrier in the direction perpendicular to the surface itself. Again, the charge can be adjusted in a way that, when it is increased by a certain amount, atoms in $|b\rangle$ would impact onto the surface, while atoms in $|a\rangle$ would remain trapped above it (Fig. 7).

For quantum information processing more sophisticated designs will be necessary. For example, we consider an atomic mirror like the one consisting of a magnetic medium with periodic magnetization along the x axis [36]. The period of the pattern, $2\pi/k_M$, can be as small as 100 nm using existing magnetic storage technologies. The modulus of the magnetic field thus generated is constant over the surface and exponentially decaying with distance z from the surface. Adding an external bias field leads to the appearance of minima along x and z, where atoms can be trapped. The spacing between two nearest minima along x is of the order of $2\pi/k_M$. With present-day technology, trapping frequencies can range from a few tens of kHz up to some MHz. By using a magnetization with two different frequency components along x, the minima show up in pairs. Microscopic electrodes can be nanofabricated on the mirror surface [7] below each pair. Charging them produces an attractive potential for atoms, giving confinement along the y direction. The barrier between two nearest wells can be lowered by increasing the charge on the corresponding electrode. We can choose, e.g., the internal states $|a\rangle \equiv |F=2, m_{\rm f}=2\rangle$ and $|b\rangle \equiv |F=1, m_{\rm f}=-1\rangle$. Note that $|a\rangle$ has an interaction with the magnetic field twice as high as $|b\rangle$. Therefore the charge can be adjusted in such a way that the barrier is removed only for atoms in internal state $|b\rangle$, but still remains in place for atoms in $|a\rangle$ [9, 11].

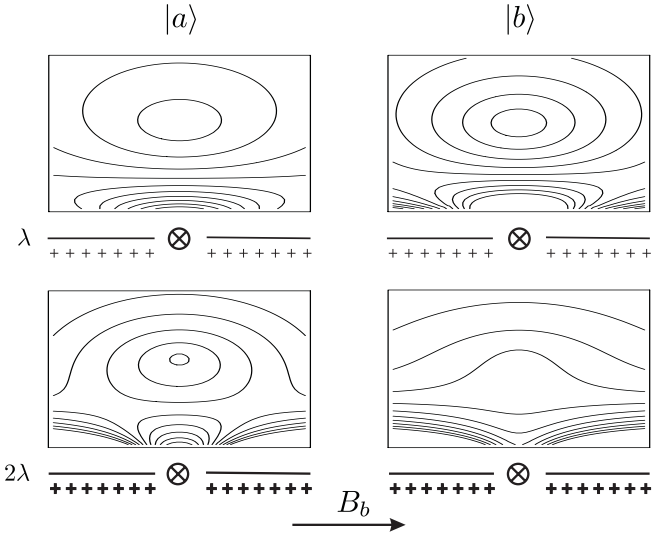

Fig. 7. State dependent potential (see text): the charged wire is parallel to the page, the side guide goes perpendicular to it. *Left (right) column* shows the total potential for atoms in state $|a\rangle = |F=2, m_{\rm f}=2\rangle$ ($|b\rangle = |F=1, m_{\rm f}=-1\rangle$). Linear charge density λ in the lower plots is twice as large as in the upper plots

1.2 Loading from large to small

The question arises as to how these atom optical circuits on a surface can be loaded with cold atoms. A possible solution could be to load cold atoms (or a BEC) into a free standing wire guide [16, 18, 19], which then transports the atoms to the surface mounted mesoscopic devices.

A different solution would be to create a reservoir of cold atoms (preferably a BEC or a degenerate Fermi gas) directly in a surface mounted Z-trap and to load the atoms from there using surface mounted atom guides.

The latter requires atoms to be loaded into chip traps. Thereby one has to solve three problems. First, to make or bring cold atoms close to the chip, second, to load the atoms into the magnetic trap on a chip, and third, to transfer them to smaller and smaller traps.

For the first step, making the cold atoms close to the chip, one has to ensure that the atoms can be laser cooled and trapped close to the surface. This requires the surface of the *Atom Chip* to be either transparent or reflecting, using a mirror MOT [38].

The second step requires a relatively strong magnetic trap into which the atoms can be loaded from the MOT and possibly further cooled by evaporation.

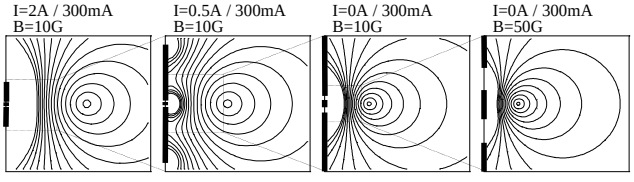

Fig. 8. Loading a microscopic atom trap (10 μm wire, trap frequency above 100 kHz and ground state size below 100 nm) from a large trap formed by two 200-μm wires. The wire for the small trap carrying 300 mA is located between the two thick wires. By ramping down the current in the thick wires the potential automatically moves closer to the surface until all the trapping is done by the thin wire and the bias field. Increasing the bias magnetic field moves the trap even closer to the surface and compresses it even more (*last graph*). Each successive picture zooms in on a small portion of the previous one, as indicated by the square

The third step requires the successive loading of smaller and smaller traps or guides to transfer the atoms from the larger to the smaller steeper trap. This loading from one trap to the next can easily be achieved by (adiabatically) ramping down the current in the thick wires of the larger trap as illustrated in Fig. 8. In the transfer from large to small, the atomic sample will be compressed.

2 Experiments

Here we give a brief overview of our experiments studying microscopic magnetic traps using free standing wires and atom chips.

All our experiments are done with laser cooled lithium atoms from a magneto-optical trap (MOT) (see Fig. 9 and [37]). Atoms from this MOT are then loaded into the guiding or trapping potentials. They move within the potential for some time and the resulting atomic distribution is studied using fluorescent light imaging.

2.1 Wire experiments

To study the basic principles of micromanipulation of atoms with small current carrying structures, we started experiments with free standing wires. The first experiments were conducted in the early 1990s and demonstrated the guiding of thermal Na atoms along a 1-m long wire. The wire was bent and the atoms were guided around a beam stop [16].

2.1.1 Wire guides. In our recent experiments, we studied guiding and trapping using current carrying wires with laser cooled Li atoms from a MOT (Fig. 10). We performed experiments studying a Kepler guide with atoms orbiting around the wire, and investigated the side guide with atoms guided in a potential minimum along the side of the wire. Thereby, the scaling laws mentioned earlier were confirmed [18–20].

Furthermore, we studied beam splitting potentials for guided atoms formed by combining two guides in the form of a Y. By controlling the current through the arms of the Y-shaped structure we can send cold atoms along either arms of the Y or into both arms simultaneously (Fig. 10b) [19].

2.1.2 Wire traps. Using a Z-shaped wire and a uniform bias field we built an Ioffe–Pritchard-type magnetic trap (Fig. 11).

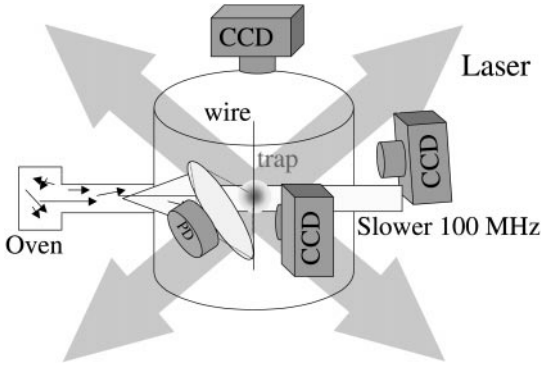

Fig. 9. The schematic setup of the experiment. The three CCD cameras allow observation of the trapped atoms from three nearly orthogonal directions

Atoms are trapped above the wire and compressed by increasing the bias field. The compression of the trap is limited by the finite size of the wire. Too strong compression moves the potential minimum into the wire. The maximum compression shown in the right pictures in Fig. 11 is loss free as we could verify from re-expanding the trap and measuring the atom number. One easily obtains trap parameters which exceed those needed for BEC with only a few Watts of power consumption. Quantitative analysis of this data verified the expected scaling properties [31].

2.2 Atom Chip Experiments

2.2.1 The Atom Chip. The *Atom Chips* we have used for our experiments are made of a 2.5-μm gold layer placed on a 0.6-mm thick GaAs substrate [39]. The chip wires are all defined by boundaries of 10-μm wide etchings in which the conductive gold has been removed. This leaves the chip as a gold mirror (with 10-μm etchings) and it can be used to reflect the laser beams for the MOT during the cooling and collecting of atoms.

In Fig. 12a we present the main elements of the chip design. Each of the large U-shaped wires, together with a bias field, creates a quadrupole field, which may be used to form an MOT on the chip as well as a magnetic trap. Both U-shaped wires together may be used to form a strong magnetic trap in order to 'load' atoms into the smaller structures, or as an on-board (i.e. without need for external coils) bias field, for guides and traps created by the thin wire running between them. The thin wires are 10-μm wide, and depending on the contact used, may form a U-shaped or a Z-shaped magnetic trap or a magnetic guide.

In addition, a U-shaped 1-mm thick wire, capable of carrying up to 20 A of current, has been put underneath the chip in order to assist with the loading of the chip. Its location and shape are identical to those of one of the 200-μm U-shaped wires and it differs only in the amount of current it can carry.

Figure 12b shows the mounted chip before it is introduced into the vacuum chamber used for atom trapping experiments.

The experimental procedure for loading cold atoms into the small traps on the chip is the following [25]:

2.2.2 Mirror MOT. In the first step typically 10^8 ^{7}Li atoms are loaded from an effusive atomic beam into a MOT (Fig. 13, reflection MOT). Because the atoms have to be collected a few millimeters away from the surface we use a 'reflection' MOT [26, 38]. Thereby, the six laser beams needed for the MOT are formed from four beams by reflecting two of them off the chip surface. Four circularly polarized light beams enter the chamber; two are counter propagating parallel to the surface of the chip, while the two others, impinging on the surface of the chip at a 45-degree angle, are reflected by the gold layer. Hence, atoms above the chip actually encounter six light beams in the correct configuration of polarisation needed for the formation of a MOT. To ensure a correct magnetic field configuration for the MOT, one of the reflected light beams has to be in the axis with the MOT coils. The top row of Fig. 13 shows, besides a schematic of the laser beams, MOT coils and the *atom chip*, a top view of the reflection MOT sitting above the chip with some of its electric connections.

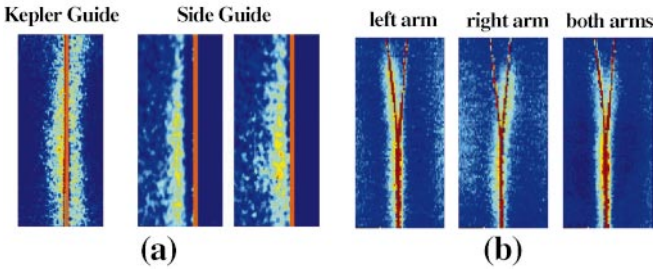

Fig. 10a,b. Wire guides for atoms: The pictures show CCD images of **a** Kepler guide and side guide for different wire currents, and **b** Atoms guided in a beam splitting potential formed by a current carrying Y wire

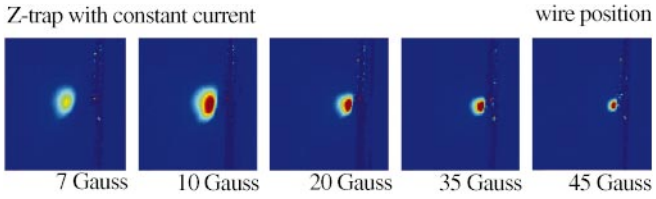

Fig. 11. Z-trap: The pictures show CCD images of atoms in a Z-trap at various stages of compression. By ramping up the bias field gradients of $\geq 500\,\mathrm{G/cm}$ were obtained. The Z-trap was made out of a 1-mm thick Cu-wire carrying 22 A of current

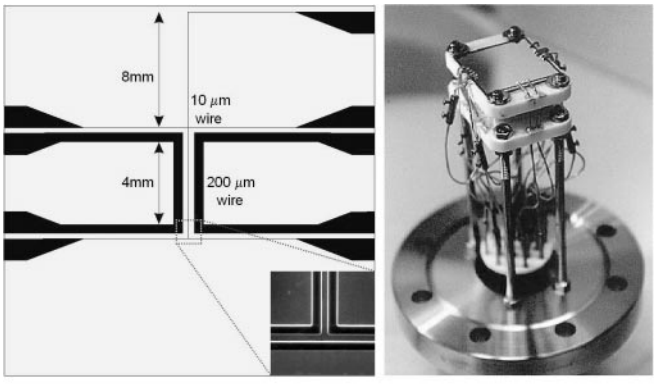

Fig. 12. a A schematic of the chip surface design. For simplicity, only wires used in the experiment are shown. The wide wires are 200 μm wide while the thin wires are 10 μm wide. The *insert* shows an electron microscope image of the surface and its 10-μm wide etchings defining the wires. **b** The mounted chip before it is introduced into the vacuum chamber

The large external quadrupole coils are then switched off while the current in the U-shaped wire underneath the chip is switched on, together with an external bias field. This forms a nearly identical, but spatially smaller, quadrupole field as compared to the fields of the large coils. The atoms are thus transferred to a secondary MOT which by construction is always well aligned with the chip (Fig. 13, U-MOT). By changing the bias field, the MOT can be shifted close to the chip surface.

2.2.3 Loading the Atom Chip. In the next step, the laser beams are switched off and the quadrupole field serves as a magnetic trap in which the low field seeking atoms are attracted to the minimum of the field (Fig. 13, U-trap). The magnetic trap is then lowered further towards the surface of the chip by increasing the bias field. Atoms are now close enough so that they can be trapped by the chip fields.

Next, a current of 2 A is sent through each of the two 200-μm U-shaped wires on the chip and the current in the U-shaped wire located underneath the chip is ramped down

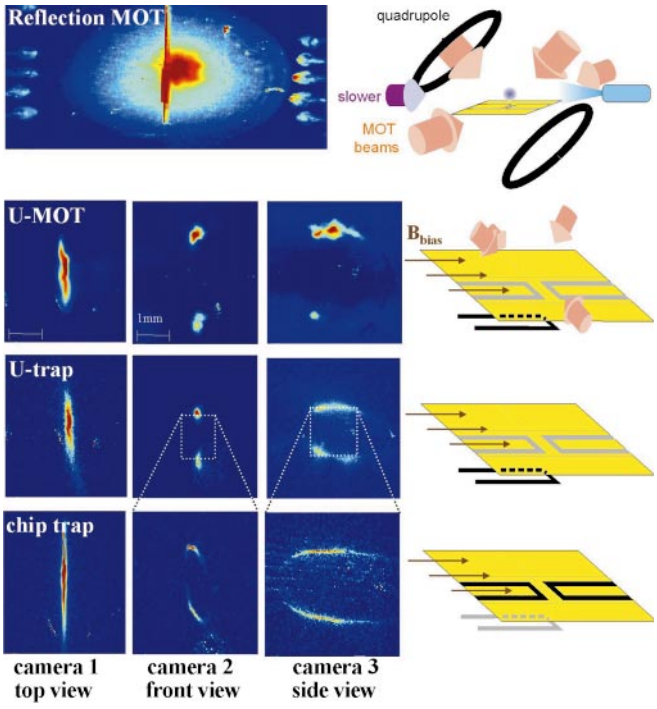

Fig. 13. Transfering cold atoms to an *Atom Chip*: column (i) shows the view from the top (*camera 1*), column (ii) the front view (*camera 2*), column (iii) the side view (*camera 3*), and (iv) a schematic of the wire configuration. Current carrying wires are *highlighted in black*. The front and side views show two images: the upper is the actual atom cloud and the lower is the reflection on the gold surface of the chip. The distance between both images is an indication of the distance of the atoms from the chip surface. The rows show the step-wise process of loading atoms onto the chip. The pictures of the magnetically trapped atomic cloud are obtained by fluorescence imaging using a short laser pulse (typically 0.5 ms)

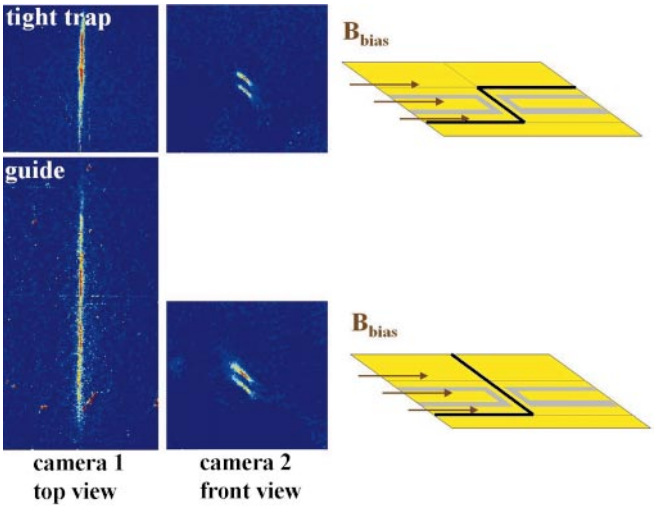

Fig. 14. Cold atoms in micro-traps and guides on an *Atom Chip*: The *top row* shows atoms in a microscopic trap 20 μm above the chip surface. The *bottom row* displays atoms propagating in a guide. Current carrying wires are *highlighted in black*

to zero. This procedure brings the atoms even closer to the chip, typically a few 100 μm, compresses the trap considerably, and transfers the atoms to a magnetic trap formed by the currents in the chip (Fig. 13, chip trap).

2.2.4 Loading smaller traps. Finally, a wire trap on the microscopic scale is loaded by first sending a current of 300 mA through the thin wire. Then the current in both the U-shaped wires is ramped down to zero (see also Fig. 8). Atoms are now typically a few tens of microns above the surface (Fig. 14, tight trap). By running the current through a longer section of the thin wire, we turn the magnetic trap into a guide, and atoms could be observed expanding along it (Fig. 14, guide). In these small traps, the atom cloud can be compressed to the point where direct visual observation is difficult. In such a case, we observe those atoms after guiding or trapping, by 'pulling' them up again away from the surface and into a less compressed wire trap (by just increasing the wire current or decreasing the bias field).

In our experiments [25] we have realized a wide variety of magnetic potentials including a 3D quadrupole for a MOT, 3D magnetic Ioffe–Pritchard-like traps, and 2D minima for guiding allowing us to easily manipulate position and width of the trapped atomic cloud. We achieved trap parameters with a transverse ground state size below 100 nm and frequencies of above 100 kHz (as required by the QIP proposals). In addition we could trap and guide atoms exclusively with the chip fields. Namely, we used the field generated by the two U-shaped wires, as an on-board bias field for the small wire trap.

Last, but not least, it has been shown that standard nanofabrication techniques and materials may be utilized to build these *Atom Chips*. The wires on the surface can stand sufficiently high current densities in vacuum and at room temperature. Together with the scaling laws of these traps, this will allow us to use much thinner wires and reach traps with ground state sizes of 10 nm and trap frequencies in the MHz range.

The above shows that the concept of an *Atom Chip* clearly works. Namely, atoms may be put close to the surface in simple magnetic and electric potentials that have the right scaling laws so that one may achieve very steep traps with small ground state size and large energy level spacing.

3 Outlook

We would like to conclude with a long term outlook: Atom optics has proven itself to be an extremely successful tool for research into the foundations of quantum theory concerning topics such as matter-wave interference, entanglement and the uncertainty principle, and for the development of technological applications such as clocks and acceleration sensors. Most of the present experiments are put together as a macroscopic apparatus from single atom optical elements, in a way similar to the first electronic devices were built from parts performing single tasks.

Integrating many elements to control atoms onto a single device, an *Atom Chip* will make atomic physics experiments much more robust and simple. This will allow much more complicated tasks in atom manipulation to be performed, in a way similar to what integration of electronic elements allowed in the development of new powerful devices.

This is of special interest since it has been suggested that the high degree of control achieved over neutral atoms and their weak coupling to the environment (long decoherence time) will allow the realization of quantum information processing (QIP).

In this work we have successfully realized the first steps of many still needed in this direction. A final integrated *Atom Chip* should have a reliable source of cold atoms with an efficient loading mechanism, single mode guides for coherent transportation of atoms, nanoscale traps, movable potentials allowing controlled collisions for the creation of entanglement between atoms, extremely high resolution light fields for the manipulation of individual atoms, and internal state sensitive detection such as cavity QED to read out the result of the processes that have occurred (e.g. the quantum computation). All of these, including the bias fields and probably even the light sources, could be on board a self-contained chip. This would involve sophisticated 3D nanofabrication and the integration of a diversity of electronic and optical elements, as well as extensive research into fundamental issues such as decoherence near a surface. Such a robust and easy-to-use device would make advances in many different fields of quantum optics possible: from applications such as clocks and sensors to implementations of quantum information processing and communication.

Acknowledgements. Atom Chips used in the preparation of this work and in the actual experiments were fabricated at the Institut für Festkörperelektronik, Technische Universität Wien, Austria, and the Sub-micron center, Weizmann Inst. of Science, Israel. We thank E. Gornik, C. Unterrainer and I. Bar-Joseph of these institutions for their assistance. We gratefully acknowledge many discussions with P. Zoller about microtraps and their application in quantum information. This work was supported by the Austrian Science Foundation (FWF), project S065-05 and SFB F15-07, the Jubiläums Fonds der Österreichischen Nationalbank, project 6400, and by the European Union, contract Nr. TMRX-CT96-0002, HPMF-CT-1999-00211 and HPMF-CT-1999-00235. B. H. acknowledges financial support from Svenska Institutet, and T. C. from Istituto Trentino di Cultura.

References

1. See for example: *Quantum Coherence in Mesoscopic Systems*, ed. by B. Kramer, NATO ASI Series B: Physics, Vol. 254 (Plenum Press 1991)
2. See for example: B.E.A. Saleh, M.C. Teich: *Fundamentals of Photonics* (Wiley & Sons 1991)
3. For an overview see: C.S. Adams, M. Sigel, J. Mlynek: Phys. Rep. **240**, 143 (1994); *Atom Interferometry*, ed. by P. Berman (Academic Press 1997) and references therein
4. A good overview of laser cooling is given in: *Laser Manipulation of Atoms and Ions*, ed. by E. Arimondo, W.D. Phillips, F. Strumia (North Holland, 1992); S. Chu: Rev. Mod. Phys. **70**, 685 (1998); C. Cohen-Tannoudji: Rev. Mod. Phys. **70**, 707 (1998); W.D. Phillips: Rev. Mod. Phys. **70**, 721 (1998)
5. M.H. Anderson, J.R. Ensher, M.R. Matthews, C.E. Wieman, E.A. Cornell: Science **269**, 198 (1995); K.B. Davis, M.-O. Mewes, M.R. Andrews, N.J. van Druten, D.S. Durfee, D.M. Kurn, W. Ketterle: Phys. Rev. Lett. **75**, 3969 (1995); M.-O. Mewes, M.R. Andrews, N.J. van Druten, D.M. Kurn, D.S. Durfee, C.G. Townsend, W. Ketterle: Phys. Rev. Lett. **77**, 988 (1996); C.C. Bradley, C.A. Sacket, R.G. Hulet: Phys. Rev. Lett. **78**, 985 (1997); see also C.C. Bradley, C.A. Sacket, R.G. Hulet: Phys. Rev. Lett. **75**, 1678 (1995). For a complete list of refer- ences see also the BEC Homepage http://amo.phy.gasou.edu/bec.html

6. J. Schmiedmayer: Habilitationsschrift, Universität Innsbruck (1996); J. Denschlag, J. Schmiedmayer: In Proceedings of the International Quantum Coherence Conference (World Scientific, Boston 1997)
7. J. Schmiedmayer: Eur. Phys. J. D **4**, 57 (1998)
8. E.A. Hinds, I.G. Hughes: J. Phys. D: Appl. Phys. **32**, 119 (1999)
9. H.-J. Briegel, T. Calarco, D. Jaksch, J.I. Cirac, P. Zoller: J. Mod. Opt. **47**, 415 (2000)
10. A. Ekert, R. Jozsa: Rev. Mod. Phys. **68**, 733 (1996)
11. T. Calarco, D. Jaksch, E.A. Hinds, J. Schmiedmayer, J.I. Cirac, P. Zoller: Phys. Rev. A **61**, 022304 (2000)
12. V.V. Vladimirskii: Sov. Phys. JETP **12**, 740 (1961)
13. J.M. Gerton, C.A. Sackett, B.J. Frew, R.G. Hulet: Phys. Rev. A **59**, 1514 (1999); E.R.I. Abraham, W.I. McAlexander, J.M. Gerton, R.G. Hulet, R. Côté, A. Dalgarno: Phys. Rev. A **55**, R3299; J. Weiner, V.S. Bagnato, S. Zilio, P.S. Julienne: Rev. Mod. Phys. **70**, 1 (1999)
14. W. Wing: Prog. Quant. Electr. **8**, 181 (1984)
15. The Earnshaw theorem can be generalized to any combination of electric, magnetic and gravitational field, as shown in: W. Ketterle, D. Pritchard: Appl. Phys. B **54**, 403 (1992)
16. J. Schmiedmayer: In XVIII International Conference on Quantum Electronics: Technical Digest, ed. by G. Magerl (Technische Universität Wien, Vienna 1992), Series 1992, Vol. 9, 284 (1992); Appl. Phys. B **60**, 169 (1995); Phys. Rev. A **52**, R13 (1995)
17. J. Schmiedmayer, A. Scrinzi: Phys. Rev. A **54**, R2525 (1996); JEOS – Quantum Semiclass. Opt. **8**, 693 (1996)
18. J. Denschlag, D. Cassettari, J. Schmiedmayer: quant-ph/9809076, Phys. Rev. Lett. **82**, 2014 (1999)
19. J. Denschlag, D. Cassettari, A. Chenet, S. Schneider, J. Schmiedmayer: Appl. Phys. B **69**, 291 (1999)
20. J. Denschlag: PhD thesis, Universität Innsbruck (1998)
21. R. Frisch, E. Segre: Z. Phys. **75**, 610 (1933)
22. J.D. Weinstein, K. Libbrecht: Phys. Rev. A **52**, 4004 (1995)
23. M. Drndic, K.S. Johnson, J.H. Thywissen, M. Prentiss, R.M. Westervelt: Appl. Phys. Lett. **72**, 2906 (1998)
24. J.H. Thywissen, M. Olshanii, G. Zabow, M. Drndić, K.S. Johnson, R.M. Westervelt, M. Prentiss: Eur. Phys. J. D **7**, 361 (1999)
25. Recently we have achieved trapping and manipulation of atoms in nanofabricated structures R. Folman, P. Krüger, D. Cassettari, B. Hessmo, T. Maier, J. Schmiedmayer: quant-ph/9912106, Phys. Rev. Lett. in print (1999). For experiment with large structures ($> 100\,\mu$m) see also: and [26–28]
26. J. Reichel, W. Hänsel, T.W. Hänsch: Phys. Rev. Lett. **83**, 3398 (1999)
27. D. Mueller, D.Z. Anderson, R.J. Grow, P.D.D. Schwindt, E.A. Cornell: Phys. Rev. Lett **83**, 5194 (1999)
28. N.H. Dekker, C.S. Lee, V. Lorent, J.H. Thywissen, S.P. Smith, M. Drndi, R.M. Westervelt, M. Prentiss: Phys. Rev. Lett. **84**, 1124 (2000)
29. E. Andersson, M.T. Fontenelle, S. Stenholm: Phys. Rev. A **59**, 3814 (1999)
30. D. Cassettari, A. Chenet, J. Denschlag, St. Schneider, J. Schmiedmayer: EQEC 98 (Glasgow 1998)
31. A. Haase, D. Cassettari, B. Hessmo, J. Schmiedmayer: submitted to Phys. Rev. A (1999)
32. The minimum of the U-trap is displaced from the central point of the bar, in a direction opposite to the bent wire leads. A more symmetric quadrupole can be created by using 3 wires in a H configuration. There the side-guide is closed by the two parallel wires crossing the central wire orthogonally. The trap is then in between the two wires, along the side guide wire
33. J. Fortagh, A. Grossmann, C. Zimmermann: Phys. Rev. Lett. **81**, 5310 (1998)
34. V. Vuletic, T. Fischer, M. Praeger, T.W. Hänsch, C. Zimmermann: Phys. Rev. Lett. **80**, 1634 (1998)
35. T.J. Davis: Quantum Semiclass. Opt. B **1**, 408 (1999)
36. T.M. Roach, H. Abele, M.G. Boshier, H.L. Grossman, K.P. Zetie, E.A. Hinds: Phys. Rev. Lett. **75**, 629 (1995); E.A. Hinds, M.G. Boshier, I.G. Hughes: *ibid.* **80**, 645 (1998); E.A. Hinds: Philos. Trans. Roy. Soc. London, Ser. A **357**, 1409 (1999)
37. The atoms are loaded into the MOT for 20 s out of an effusive beam at a red laser detuning of 25 MHz and a total laser power of about 150 mW. An electro-optic modulator produces sidebands of 812 MHz (30%) one of which is used as a repumper. To increase the loading rate we use an additional slower beam (20 mW, 100 MHz red detuned) directed through the MOT into the oven. The MOT is typically 1 mm in diameter (FWHM) and has a temperature of $T \sim 200\,\mu$K which corresponds to a velocity of about 0.5 m/s. For a detailed description see [19, 20]
38. K.I. Lee, J.A. Kim, H.R. Noh, W. Jhe: Opt. Lett. **21**, 1177 (1996)
39. The chip is produced using standard nano-fabrication methods. A detailed account will be given in: T. Maier et al.: to be published